



REQUIRED STRENGTH AND STIFFNESS OF DISSIPATIVE BRACING SYSTEMS FOR THE PASSIVE CONTROL OF FRAMED STRUCTURES LOCATED ON SOFT SOIL

Juan Enrique MARTINEZ-RUEDA¹ and Yazmin CABRERA-GARCIA²

SUMMARY

This article introduces design rules to estimate the required strength and stiffness of dissipative bracing used for the seismic design or redesign of framed structures. These rules are calibrated by a parametric study on the inelastic response of SDOF systems under the action of scaled accelerograms recorded on soft soil. The proposed rules are sensitive to both the period and the seismic coefficient of the frame where the dissipative bracing is installed, and can be used for the preliminary design of dissipative bracing to impose a passive control on the ductility demand of framed structures.

INTRODUCTION

A framed structure with a bracing system that incorporates hysteretic devices (dissipative bracing) is now generally accepted as an efficient earthquake resistant system. The dissipative bracing protects the structure from damage by dissipating energy by hysteresis in yielding or friction in special devices referred to as hysteretic devices. Using this approach the energy dissipation characteristics of the structure can be more easily detailed and optimized.

The technology for hysteretic devices has evolved successfully during the last two or three decades [1], and has resulted in several options the designer can choose from to create a dissipative bracing with optimum hysteretic behavior. However, the fundamental problem of how to choose the global properties of the dissipative bracing in terms of its strength and stiffness remains in need of practical solutions. In general, a formal evaluation of the effectiveness of a dissipative bracing installed into a framed structure requires of elaborate and time-consuming nonlinear seismic analyses. This process includes the consideration of several analytical models with different combinations of strength and stiffness for the dissipative bracing under the action of several earthquake records. Normally, several iterations are needed to arrive at the final strength and stiffness of the dissipative bracing. Accordingly, the development of design formulae to estimate the required properties of dissipative bracing is an active research area of practical interest.

¹ Civil Engineering Division, School of the Environment, University of Brighton, UK.

² Instituto Tecnológico y de Estudios Superiores de Monterrey, Zacatecas, Mexico.

Along the years, several studies to define the required properties of dissipative bracing have been conducted [e.g. 2,3]. This research has given significant insight into the main parameters controlling the efficiency of dissipative bracing in relation to the properties of the framed system where the bracing is installed. However, most of previous studies are limited because they have considered just one structure, one natural accelerogram, or several artificial accelerograms.

More recently, Cabrera-Garcia and Martinez-Rueda [4] conducted a study on the effect that the strength and the stiffness of dissipative bracing have on the reduction of ductility demands of framed structures subjected to the action of twenty natural accelerograms recorded on stiff soil. This study revealed the adequacy of a parametric study to propose and calibrate design rules for the required strength and stiffness of dissipative bracing. Although design rules sensitive to the strength and stiffness of the framed structure were identified, the rules were not very versatile. In fact, the rules were constrained to many subregions of the full range of periods and strengths considered in the study.

Objectives and scope

This paper introduces a new methodology to calibrate the strength and stiffness of a dissipative bracing to achieve a target ductility demand under seismic loading. The type of structure under study is a dual system formed by a frame component and a bracing component. The seismic input consists of a family of natural accelerograms recorded on soft soil scaled to different seismicity levels.

The frame component consists of a framed structure with earthquake response dominated by bending in its members. The bracing component consists of a dissipative bracing system that can be introduced according to two possible design scenarios under the anticipated seismic actions. The first scenario considers the redesign of an existing framed structure (also called original or virgin structure) where dissipative bracing is introduced to improve seismic performance. The designer has control over the properties of the dissipative bracing including its ductility capacity. The main design objective is to ensure that the ductility capacity of the existing frame is not exceeded. Another possibility within this scenario is the conversion of conventional bracing into dissipative bracing. The second scenario includes the design of a new framed structure with dissipative bracing where the designer has control over the ductility capacity of both the framed structure and the dissipative bracing.

PARAMETRIC STUDY

Modeling assumptions and method of analysis

The structures under study were idealized as nonlinear SDOF systems like that shown in Figure 1. The system is subjected to seismic excitation in terms of the ground acceleration $\ddot{u}_g(t)$, and is formed by the assembly of two nonlinear springs and a dashpot, all connected in parallel to the mass of the system M . The total system stiffness is made of two components. The spring with stiffness k_o accounts for the stiffness of the frame component (original structure when dealing with seismic redesign). The spring with stiffness k_d represents the contribution of the dissipative bracing. Structures with and without dissipative bracing were assumed to have a viscous damping ratio of 5%.

Figure 2 shows the envelopes of lateral strength for the two global components of the structures under study. The initial stiffness of the framed structure and the bracing system are denoted by k_y and k_{yd} , respectively. As a result of the interaction between the framed structure and the dissipative bracing the initial stiffness and effective yield strength of the upgraded structure are $k_y + k_{yd}$ and $H_y + H_{yd}$, respectively. The modeling assumptions summarized by Figures 1 and 2 are similar to those adopted by Ciampi et al. [3] for the study of dissipative bracing using artificial accelerograms; however these authors

neglected the capacity of the frame component to exhibit hardening and considered the response of this component as elastic-perfectly plastic.

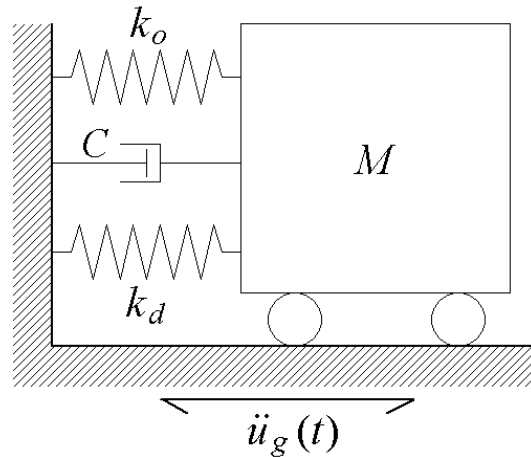


Figure 1. Idealization of a framed system with dissipative bracing as a nonlinear SDOF system with two stiffness components.

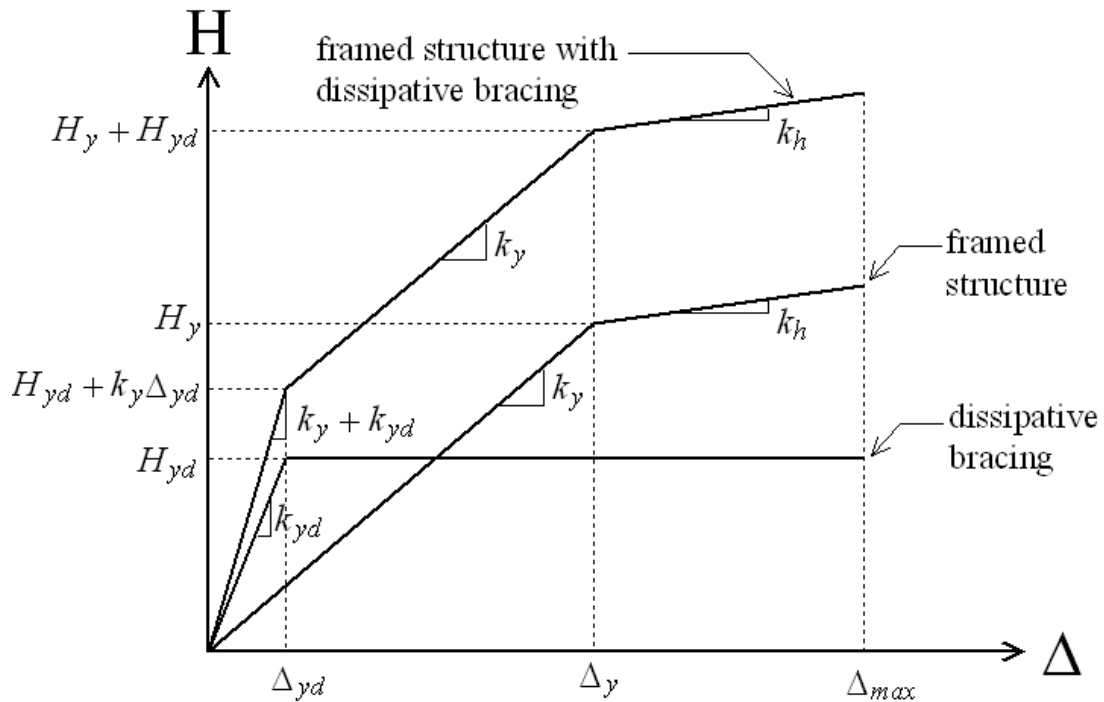


Figure 2. Strength envelope in terms of the lateral strength H vs. lateral displacement Δ for a framed structure with dissipative bracing idealized as an inelastic SDOF system.

The computer code INPARSYS [5] was expressly implemented to do the time-history analyses of the inelastic SDOF system of Figure 1. This code solves the equation of motion given as:

$$M\ddot{u}(t) + C\dot{u}(t) + ku(t) = -M\ddot{u}_g(t) \quad (1)$$

where the lateral stiffness k takes into account the contribution of the two springs depicted in Figure 1:

$$k = k_o + k_d \quad (2)$$

The stiffness k changes with time as a function of the history of displacements imposed by the ground motion and the hysteretic models adopted for the springs. A bilinear model with kinematic hardening was used for both springs. An elastic perfectly plastic envelope was assumed for the modeling of the dissipative bracing as illustrated in Figure 2. This assumption is consistent with the expected performance of a bracing system relying on properly designed hysteretic devices [1]. For the framed structure the postyield stiffness k_h was given the typical value of 5% of the initial stiffness k_y .

The Runge-Kutta method is adopted in INPARSYS to solve numerically the equation of motion. This method offers a true fourth-order accuracy in the evaluation of both displacements and velocities [6], and it has been shown to have better performance than the usually adopted Newmark's method in terms of accuracy, stability and convergence [7].

Variables considered in the parametric study

To have a good mixture of relevant ingredients of seismic response, the following parameters were selected for the study:

- the initial stiffness of the framed component k_y
- the yield strength of the framed component H_y
- the initial stiffness of the dissipative bracing k_{yd}
- the yield strength of the dissipative bracing H_{yd}
- the variability of the seismic input
- the intensity of the seismic input

As explained in more detail below, the properties of the structures with dissipative bracing were referred to those of the structures without devices.

Characterization of strength and stiffness

The strength of the structures without dissipative bracing was characterized by the seismic coefficient C_y of the frame component defined as:

$$C_y = \frac{H_y}{Mg} \quad (3)$$

where H_y is the yield strength of the framed structure and g is the acceleration of gravity.

The period of the structures was expressed in terms of the yield period of the frame without dissipative bracing T_y ; this is given by:

$$T_y = 2\pi \sqrt{\frac{M}{k_y}} \quad (4)$$

The gain in strength and stiffness resulting from the installation of dissipative bracing was defined by the factors α_k and α_h , respectively:

$$\alpha_h = \frac{H_{yd}}{H_y} \quad (5)$$

$$\alpha_k = \frac{k_{yd}}{k_y} \quad (6)$$

It is important to note that structures without dissipative bracing can be alternatively visualized as having $\alpha_k = 0$ or $\alpha_h = 0$.

Seismic input

To account for the variability of the seismic input, the family of 10 strong ground motion records shown in Table 1 was used for the time-history analyses. The selection of the records was guided not only by their strong motion characteristics but also by their predominant period T_d . For each accelerogram, T_d was defined as that period associated with the frequency of highest amplitude of the Fourier spectrum. Table 1 shows that there is a good spread of the T_d values over the range of structural periods T_y covered in the study.

Table 1. Catalogue of strong motion accelerograms recorded on soft soil.

Country	Date [m/d/y]	M_s	D_e [km]	Station	Component	PGA [g]	T_d [sec]
URSS	12/07/88	6.8	20	Gukasyan	Lateral	0.182	0.40
Italy	04/15/78	5.8	11	Patti	Lateral	0.073	0.52
Japan	01/16/95	7.0	135	Hikone	Transversal	0.140	0.59
Mexico	06/15/99	6.5	58	Chilpancingo UAG	Transversal	0.104	0.70
USA	10/18/89	7.1	14	Sn Fco. Intl. Airport	Transversal	0.235	0.93
Chile	03/03/95	7.8	25	Llaylla	Lateral	0.076	1.00
Mexico	09/14/95	7.2	121	Chilpancingo UAG	Transversal	0.088	1.29
Greece	02/24/81	6.7	4	Xylocastro	Lateral	0.292	1.58
Mexico	06/15/99	6.5	200	Alameda	Lateral	0.030	1.76
Mexico	09/19/85	8.1	400	SCT	Transversal	0.172	2.05

To account for the different levels of intensity expected in the seismic input, the above accelerograms were scaled to three seismicity levels denoted as Z1, Z2 and Z4; these correspond to the intensity of the design spectrum for soft soil anchored at peak ground acceleration (PGA) levels equal to 0.1g, 0.2g and 0.4g, respectively. The shape of the design spectrum adopted in the study was that of Eurocode 8 (EC8) [8] for soft soil.

The adopted scaling procedure is based on the original proposal of Martinez-Rueda [9] subsequently refined to account for type of soil and type of hysteretic response [10]. This procedure imposes equality between the pseudovelocity (PSV) spectrum of the accelerogram and the PSV spectrum derived from the adopted design spectrum. Figure 3 shows an example of the variability of the seismic input in terms of a comparison between the *PSV design spectrum* (PSV spectrum derived from the PSA design spectrum)

and the PSV response spectra of the scaled accelerograms. It is observed that the PSV design spectrum is effectively enclosed by the family of response spectra, despite the marked differences between the smooth shape of the PSV design spectrum and the irregular shape of the response spectra.

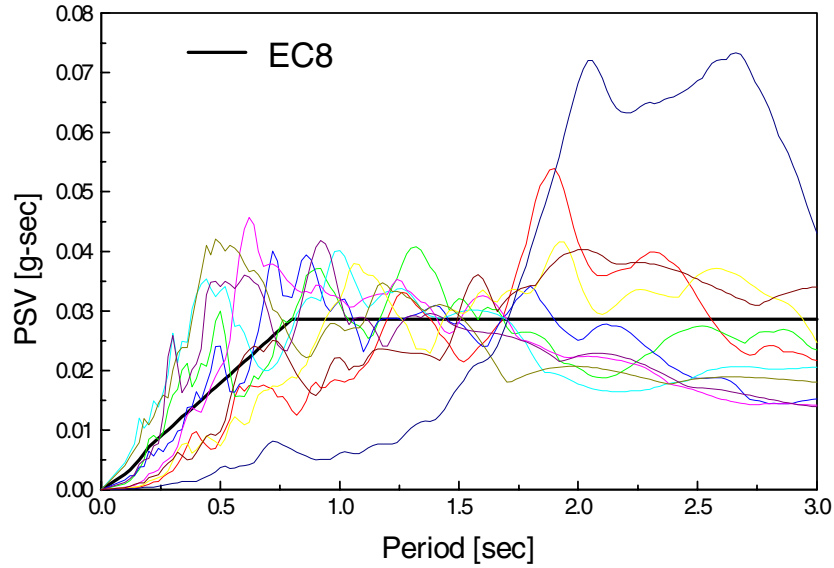


Figure 3. Comparison between the PSV spectrum associated to the EC8 design spectrum for soft soil and the PSV response spectra of the scaled accelerograms for a structure with $C_y = 0.1$ and $T_y = 0.5$ sec.

It is important to visualize that the family of structures were not specifically designed for the above spectra. Instead, different combinations of strength and period of vibration were considered and the seismic demands were assessed using the scaled accelerograms. This with the aim of producing a good scatter of results in terms of seismic demands for structures with and without dissipative bracing for realistic levels of ductility demands.

ANALYSIS OF RESULTS

Total number of analyses and interpretation

The combinations between the discrete values for C_y , T_y , α_k , α_h and the scaled accelerograms for the seismicity levels resulted in 151,500 analyses (150,000 analyses for structures with dissipative bracing plus 1500 analyses of structures without dissipative bracing). These results provided the raw data for the calibration of design rules for the properties of the dissipative bracing as described in the following sections. In all cases ductility demand was reported as that inflicted on the framed structure. This allowed the assessment of ductility demand reduction in the most vulnerable component of the system. Accordingly, for each of the above analyses the ductility demand imposed on the frame component of structures with ($\mu_{\Delta r}$) and without ($\mu_{\Delta o}$) dissipative bracing was evaluated as:

$$\mu_{\Delta o} = \frac{\Delta_{\max o}}{\Delta_y} \quad (7)$$

$$\mu_{\Delta r} = \frac{\Delta_{\max o}}{\Delta_y} \quad (8)$$

where $\Delta_{\max o}$ is the maximum displacement of the structure without dissipative bracing; $\Delta_{\max r}$ is the maximum displacement of the structure with dissipative bracing; Δ_y is the yield displacement of the frame component.

The ductility demands reported below correspond to mean values for a given combination of C_y , T_y , α_k and α_h under the action of the accelerograms of Table 1 scaled to a given seismicity level.

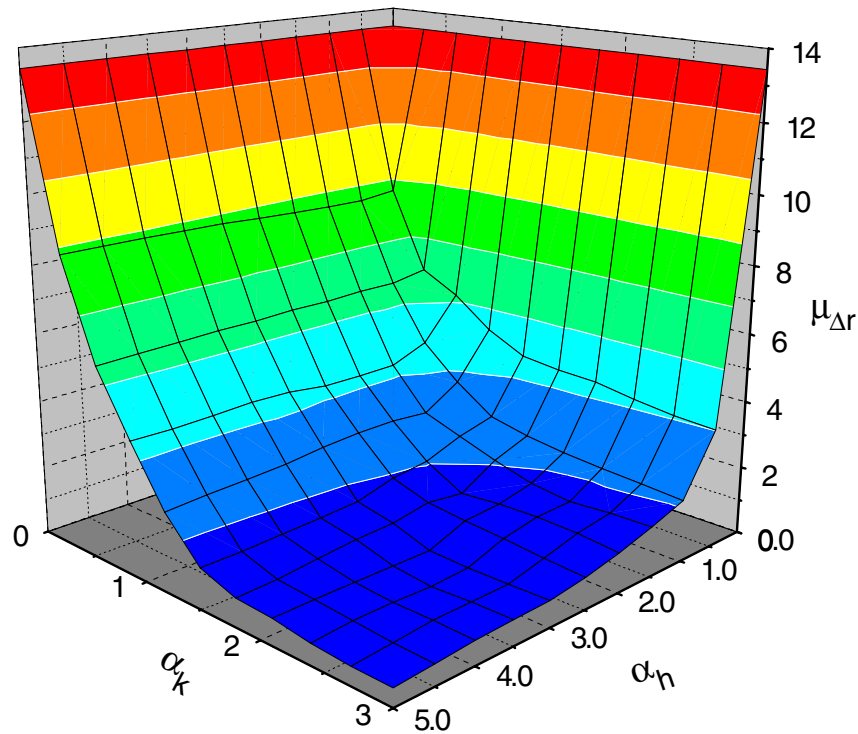


Figure 4. Example of a surface of ductility demands for a framed structure with dissipative bracing. This surface corresponds to a structure with $C_y = 0.1$, $T_y = 0.2$ sec for seismicity Z2.

Figure 4 shows a typical surface of ductility demands for a given structure in its original and redesign condition. This surface summarizes the results of 1010 analyses that correspond to the structure with dissipative bracing for all the combinations of α_k and α_h (10×10) and the structure without dissipative bracing (10), all under the action of the 10 natural accelerograms ($10 \times 10 \times 10 + 10 = 1010$) of Table 1, scaled to be consistent with the seismicity Z2. It is observed that the structure without dissipative bracing experiences the maximum ductility demand. This structure corresponds to points of the surface with $\alpha_k = 0$ or $\alpha_h = 0$, *i.e.* the horizontal lines intersecting planes $\alpha_k \mu_{\Delta r}$ and $\alpha_h \mu_{\Delta r}$. Different combinations of $\alpha_k \neq 0$ and $\alpha_h \neq 0$ result in a reduction of the above maximum ductility demand. In fact, the largest reduction of ductility demand corresponds to the point where the dissipative bracing has the maximum values for strength and stiffness considered in the study. It is also evident that the reduction

of ductility demand occurs in a nonlinear fashion for increasing values of α_k and α_h . There was not a single case detected where an increase of ductility demand resulted from the installation of the dissipative bracing. In other words, the additional stiffness and supplemental hysteretic damping provided by the dissipative bracing proved to be always beneficial.

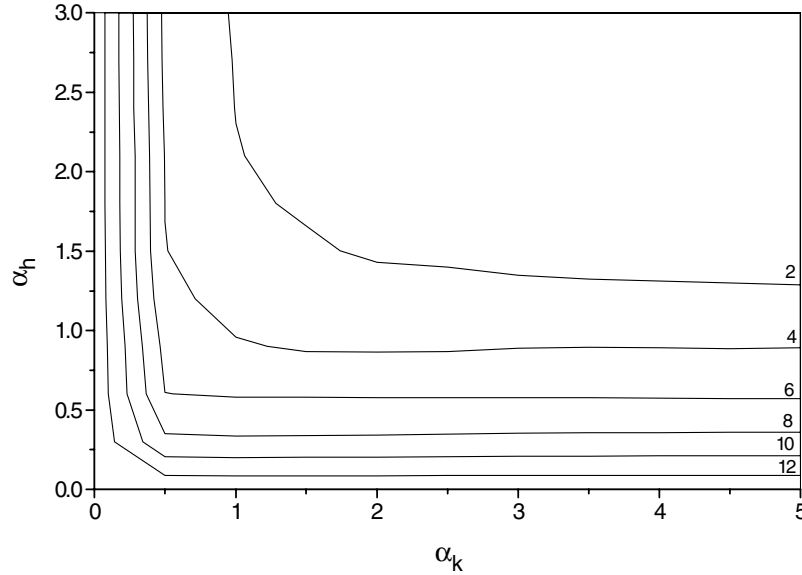


Figure 5. Contours of constant ductility demand for $C_y = 0.1$, $T_y = 0.2$ sec and seismicity Z2.

The surface of ductility demands also reveals that, in theory, there is an infinite number of combinations of strength and stiffness of the dissipative bracing to achieve a target ductility demand in the framed structure. The contours of constant ductility demands (or target ductility demands) of the above surface are shown in Figure 5. This figure is representative of the trends observed for other combinations of C_y , T_y and Z. The contours appear to follow hyperbolic relations with asymptotic lines parallel to the axes $\alpha_k = 0$ and $\alpha_h = 0$. In general, for the contours shown, values of α_k in excess of 3 correspond to regions of the contours where α_h tends to a local minimum.

Criterion to estimate an optimum combination of strength and stiffness of the dissipative bracing

The strength and stiffness of dissipative bracing are properties that are dependent of each other; hence, for a given contour of target ductility demand it is difficult to assess the optimum combination between α_k and α_h without taking into account the cost of the dissipative bracing. For simplicity, it was considered that a good estimate of the optimum combination between α_k and α_h corresponds to the point of the contour closest to the origin. In mathematical terms, this assumed optimum combination corresponds to the minimum value of r defined by:

$$r = \sqrt{\alpha_k^2 + \alpha_h^2} \quad (9)$$

For a given target ductility demand, the optimum combination of α_k and α_h values that lead to a minimum value of r in eq.(9) are denoted as α_k^* and α_h^* .

Another alternative to estimate an optimum combination of α_k and α_h values consists of locating the point demarking the beginning of a sensibly flat region of the contour where α_h tends to a minimum. In other words, this point corresponds to the minimum value of α_k for which α_h tends to a minimum. This criterion is denoted here as the *criterion of low sensitivity to the stiffness of the dissipative bracing*, and is based on the assumption that the most expensive property of the dissipative bracing is its strength. Garcia-Cabrera and Martinez-Rueda [4] have followed this criterion while assessing the efficiency of dissipative bracing for structures on stiff soil; however in a number of cases there was no clear indication of a sensibly flat contour region, and therefore uncertain extrapolation is needed beyond the maximum value considered practical for redesign purposes ($\alpha_k = 5$). Nevertheless, there is a small difference between the optimum α_h values predicted by eq. (9) and those identified by the criterion of low sensitivity to the stiffness of the dissipative bracing. Also, the α_k values predicted by eq. (9) are consistently smaller than those associated with the criterion of low sensitivity to the stiffness of the dissipative bracing.

Identification of analytic models to predict optimum properties of dissipative bracing

For each optimum combination of α_k and α_h values, the effectiveness of the dissipative bracing in the reduction of ductility demands of the framed structure was evaluated in terms of the ductility demand ratio μ_n defined by:

$$\mu_n = \frac{\mu_{\Delta r}}{\mu_{\Delta o}} \quad (10)$$

Accordingly, a theoretical value of μ_n equal to one indicates a null reduction ($\mu_{\Delta o} = \mu_{\Delta r}$) of ductility demand. This is equivalent to the case of having the frame without devices; condition that can be alternatively expressed as $\alpha_k^* = 0$ or $\alpha_h^* = 0$.

Only contours of ductility demands equal to 1, 2, 3, 4, 5 and 6 were considered in the analysis of the effectiveness of the dissipative bracing at optimum α_k and α_h values. Figure 6 gives examples of observed relations α_k^* vs. μ_n and α_h^* vs. μ_n which reveal nonlinear trends. The scattered data of this figure corresponds to α_k^* and α_h^* values obtained by the analysis of the points of the contours with coordinates defined by the discrete values of α_k and α_h considered in the study. No smoothing of the contours by curve fitting was applied. It is estimated that a curve fitting of the contours to define more precise values of α_k^* and α_h^* would improve the degree of association between the variables involved in the analytical models proposed below.

For simplicity, a curve-fitting procedure was applied to the scattered data in terms of the following analytical models:

$$\alpha_k^* = A_k (\mu_n - 1)^2 \quad (11)$$

$$\alpha_h^* = A_h (\mu_n - 1)^2 \quad (12)$$

where A_k and A_h are calibrated curve-fitting constants that minimize the error between the observed data and the proposed analytical models, for results corresponding to a given combination of C_y and T_y .

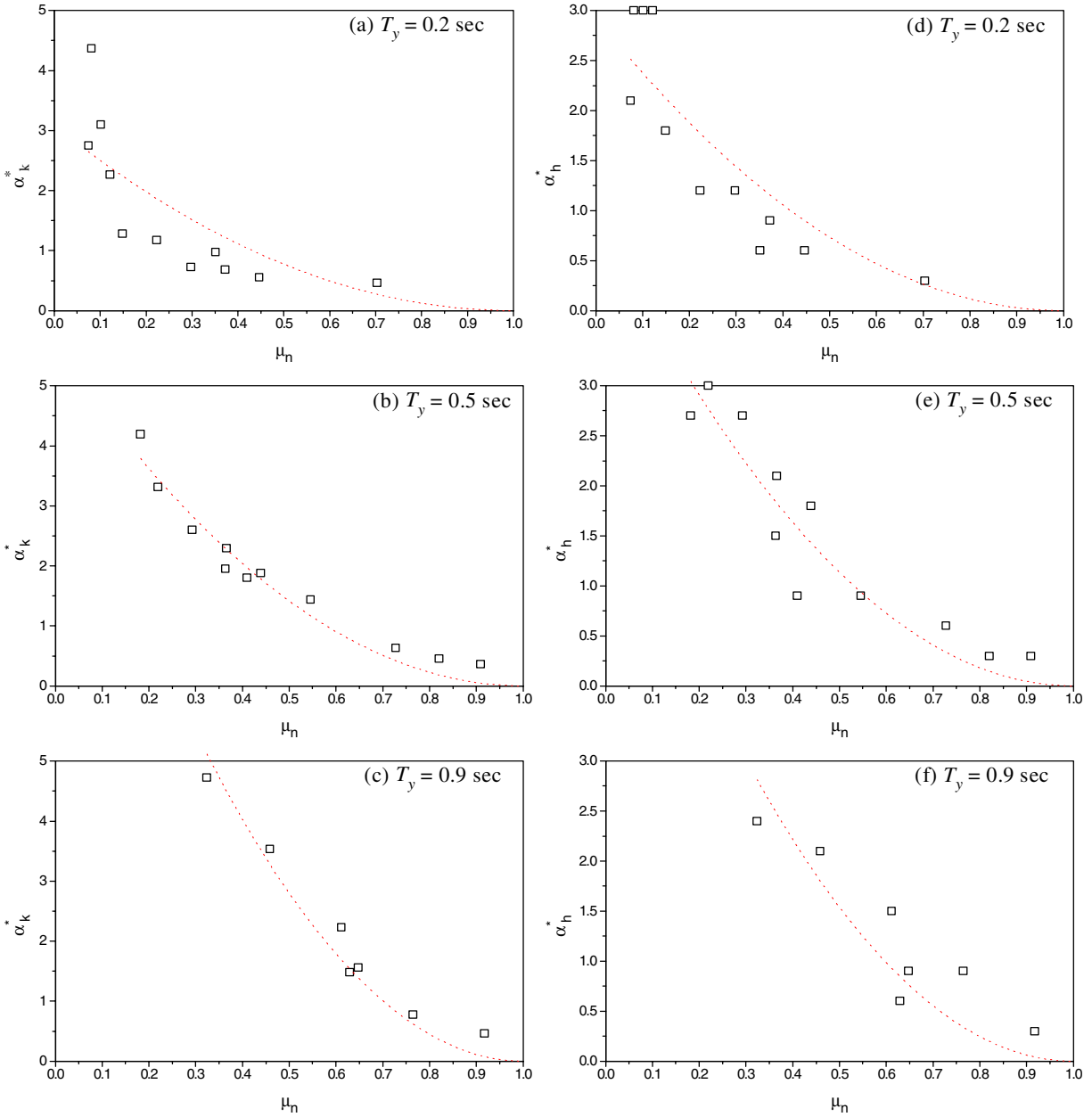


Figure 6. Examples of μ_n vs. α_k^* and μ_n vs. α_h^* relationships for $C_y = 0.1$.

It is important to observe that the above proposed nonlinear models for α_k^* and α_h^* are consistent with the expected trend for the variables involved, *i.e.* both α_k^* and α_h^* are equal to zero when μ_n is equal to one. Different degrees of dispersion, ranging from good to acceptable, between the predictive eqs. (11)-(12) and the scattered data were observed. Considering that the aim of these equations is the estimation of the required strength and stiffness of the dissipative bracing for preliminary analysis, the degree of association between the observed values of α_k^* and α_h^* and the proposed analytical models was considered adequate. Furthermore, it is argued that the uncertainties involved in inelastic seismic response cannot be reduced or removed by using a more elaborate analytical model for the curve-fitting.

Figure 7 exemplifies observed relations T_y vs. A_k and T_y vs. A_h for a given seismic coefficient C_y . The same trends, linear for T_y vs. A_k and nonlinear for T_y vs. A_h , were observed for all the C_y values.

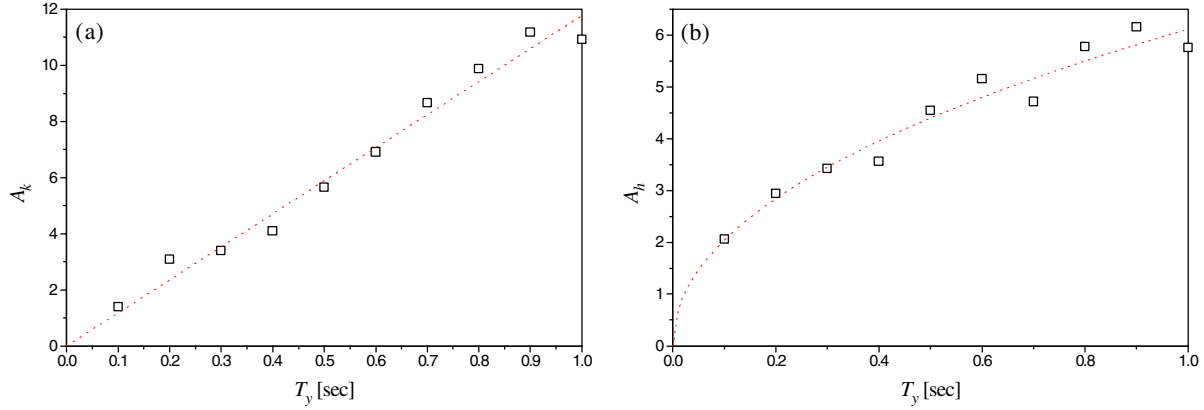


Figure 7. Observed relations T_y vs. A_k and T_y vs. A_h and adopted curve fitting models for $C_y = 0.1$

A framed structure with $T_y = 0$ can be analytically considered as a structure with infinite strength and infinite stiffness and hence it requires no reduction of ductility demands. Accordingly, for $T_y = 0$ A_k and A_h must be zero so that, in turn, α_k^* and α_h^* in eqs. (11)-(12) are predicted as zero. To be consistent with the above constrains the following models for the estimation of A_k and A_h were proposed based on a curve-fitting process:

$$A_k = m_k T_y \quad (13)$$

$$A_h = H_1 T_y^{H_2} \quad (14)$$

Table 2. Summary of coefficients in eqs. (13)-(14)

C_y	m_k	H_1	H_2
0.1	11.78	6.12	0.48
0.2	10.38	4.60	0.41
0.3	9.59	3.86	0.54
0.4	9.27	3.70	0.53
0.5	8.41	3.79	0.72

Table 2 includes the coefficients m_k , H_1 and H_2 of eqs. (13)-(14) that were evaluated for each seismic coefficient C_y . In general, good agreement was observed between the observations and the proposed models for A_k and A_h for all the values of C_y . An attempt was made to propose models for m_k , H_1 and H_2 as a function of C_y ; however, it was concluded that these models would be unreliable in terms of

both the observed reduced degree of association between the variables involved and the reduced number of points to be fitted.

Application sequence of the proposed design rules

To visualize the application of the proposed design rules for dissipative bracing, it is suggested that the following sequence is adopted.

1. Identify the frame component and the bracing component of the structure under analysis
2. Estimate the properties of the frame component: C_y, T_y
3. Estimate the ductility demand of the structure consisting of the frame component only.
4. Select a target ductility demand for the frame component consistent with its ductility capacity
5. Calculate the required ductility ratio μ_n using eq. (10)
6. Calculate the coefficients A_k and A_h using eqs. (13) and (14) and Table 2
7. Calculate the required non-dimensional strength and non-dimensional stiffness of the dissipative bracing in terms of the optimum values of α_k and α_h given by eqs. (11) and (12)
8. Calculate the required strength H_{yd} and the required stiffness k_{yd} of the dissipative bracing using eqs.(5) and (6) for $\alpha_k = \alpha_k^*$ and $\alpha_h = \alpha_h^*$.

Once the components (bracing members and hysteretic devices) of the dissipative bracing have been designed to meet the requirements defined by step 8 above, it is recommended to verify the adequacy of the design by conducting a nonlinear analysis of the complete structure. This can be done using a three-dimensional model of the structure. The use of at least four natural accelerograms properly scaled to be consistent with the design spectrum is also recommended. A short iterative procedure (starting with the preliminary values obtained in step 8 above) to refine the properties of the dissipative bracing could follow if considered necessary.

CONCLUDING REMARKS

This paper demonstrated the feasibility of the calibration of practical design rules for dissipative bracing based on a parametric study. The methodology developed for the calibration of the design rules was successful in accounting for the main parameters of the seismic response of framed structures with dissipative bracing. Accordingly, the proposed design rules are sensitive to the strength and stiffness of the framed structure where the dissipative bracing is installed. It is believed that the involvement in the above methodology of both reliability concepts and use of site-specific natural accelerograms can lead to the proposal of code design equations for dissipative bracing.

It can also be concluded that the proposed design rules have ingredients of a displacement-based design method since the designer must specify the target ductility demand of the framed structure. On the other hand, it is recognized that the successful application of the proposed design rules still depends on the ability of the designer to idealize a real multidegree of freedom structure as an equivalent SDOF system. For regular structures, rules to generate this equivalent model are already available under the umbrella of displacement-based design principles.

Finally, it should be kept in mind that the proposed design rules were calibrated for structures located on soft soil. Extrapolations to other soil conditions must be conducted with caution. An extension of this research work to cover rock and stiff soils is currently underway.

ACKNOWLEDGEMENTS

The initial stage of the research reported in this article was conducted by the authors at their former institution (UAEM, Mexico) with support from CONACYT.

REFERENCES

1. Martinez-Rueda J.E. "On the evolution of energy dissipation devices for seismic design." *Earthquake Spectra* 2002; 18(2): 309-346.
2. Filiatrault, A. & Cherry, S. "Seismic design spectra for friction-damped structures." *Journal of Structural Engineering*, ASCE 1990; 116(5): 1334-1355.
3. Ciampi, V., De Angelis, M. and Paolacci, F. "On the seismic design of dissipative bracing for seismic protection of structures." *Proceedings 2nd European Conference on Structural Dynamics*, Trondheim, Norway, 1993: 153-160.
4. Cabrera-Garcia, Y. and Martinez-Rueda, J.E. "Parametric study of bracing systems with hysteretic devices." *CDROM Proceedings 13th Mexican Conference on Seismic Engineering (in Spanish)*, SMIS, Mexico, 2001.
5. Martinez-Rueda J.E. "Analytic and experimental study of energy dissipation devices of low invasivity." *CONACYT Research Report 31256U (in Spanish)*, Mexico, 2002.
6. Berg, G.V. "Elements of structural dynamics." Prentice Hall 1989.
7. Chan, S.P. "Comparison of step-by-step methods for analyzing the dynamic response of structures" *PhD Thesis*, University of Illinois, Urbana, 1953.
8. Eurocode 8: Design provisions for earthquake resistance of structures - Part 1: General Rules. *European Committee for Standardization*, 1995.
9. Martinez-Rueda J.E. "Scaling procedure for natural accelerograms based on system of spectrum intensity scales." *Earthquake Spectra* 1998; 14(2): 135-152.
10. Martinez-Rueda J.E. "Charaterization of seismic input and its application in displacement-based design." *UAEM Research Report 1341/99 (in Spanish)*, Mexico, 2002.